ACS OMEGA

Open Access

http://pubs.acs.org/journal/acsodf

Article

Examination of the Factors Inhibiting CO_2 Adsorption on Coal: A Case Study from Shallow-Depth Low-Rank Coal Seams

Published as part of ACS Omega virtual special issue "CO2 Geostorage".

Theodora Noely Tambaria,* Yuichi Sugai, and Ferian Anggara

Cite This: *ACS Omega* 2023, 8, 42329−42339

Read Online

ACCESS | Metrics & More | Article Recommendations

ABSTRACT: Understanding the inhibitory factors affecting the adsorption of CO_2 on low-rank coal from shallow-depth coal seams is essential to identify potential coal seams for CO_2 sequestration. The CO_2 adsorption capacity of shallow-depth coals was measured at a low pressure on raw and dry coals. The samples were also prepared for organic analyses, scanning electron microscopy analyses, and low-temperature nitrogen adsorption analyses to evaluate the CO_2 adsorption and identify the inhibitory factors. An investigation was conducted to determine how CO_2 adsorption occurs on coal by fitting experimental data to adsorption isotherm models, followed by analyzing the results based on the statistical analysis. In addition, this study used Henry's law, surface potential, and Gibbs free energy to identify the adsorption inhibitor between CO_2 and coal. The CO_2 adsorption experiment was conducted on raw coal with a moisture content of 15.18−20.11% and dry coal with no moisture. The experimental data showed that the CO_2 adsorption capacity in dry coal was 1.6−1.8 times greater than that in raw coal. A fitting graph between the adsorption data and the isotherm model indicated that CO_2 adsorption on coal occurred on monolayers and multilayers under raw and dry conditions. Statistical evaluation of the adsorption isotherm models showed that the Langmuir and Freundlich models aligned more closely to the experimental data. According to this result, low-pressure adsorption of CO_2 on coal occurred in monolayers and multilayers under raw and dry conditions. Coal containing a high huminite content had a higher potential for CO_2 adsorption, and the drying increased the positive relationship. On the other hand, coal containing high inertinite content inhibited CO_2 adsorption onto the coal, but the drying process did not adversely affect CO_2 adsorption. Furthermore, coal with high moisture and inertinite content inhibited the affinity, accommodation, and spontaneous CO_2 adsorption onto the coal. CO_2 adsorption could lead to swelling, but moisture loss opened more sites and micropores, resulting in the swelling effect not closing all micropores in dry coal. Based on these results, coal seams with low moisture and inertinite content are the most promising for CO_2 adsorption. Altogether, this study provides an understanding of the percentage of inhibitor factors that affects CO_2 adsorption on low-rank coal from shallow depths, which may lead to different CO_2 adsorption capacities.

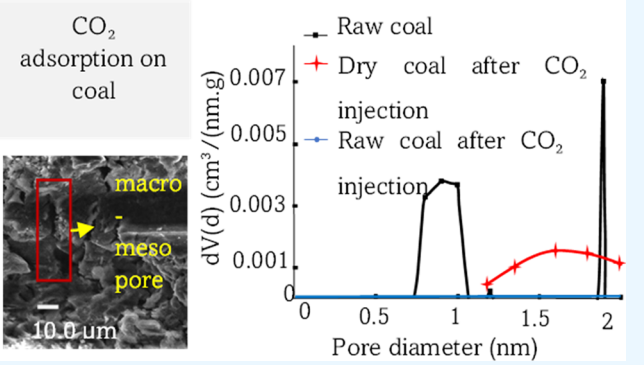

1. INTRODUCTION

Geological sequestration of CO_2 in deep unmined coal seams is one of the most innovative strategies for reducing greenhouse gas emissions. The adsorption of CO_2 on coal not only provides carbon storage but also increases coal bed methane production through its small kinetic diameter, which enables it to replace existing methane at the micropores.[1,2] It has been estimated that the worldwide potential for CO_2-ECBM (enhanced coal bed methane) amounts to 150 Gt CO_2.[3]

Studies have shown that coal extracted from deep coal seams has the highest capacity for CO_2 adsorption.[4,5] Injecting CO_2 into these deeper coal seams requires high pressure and temperature, resulting in complex interactions between the coal and gas.[6] However, increasing the injection pressure or high temperature did not improve the methane desorption rate from coal.[7] To address this issue, a new methodology was proposed, which involves ex situ dissolution of CO_2 to make its transfer easier and increase the security of geological sequestration.[8] However, this method caused problems such as shrinkage of

Received: June 28, 2023
Revised: October 17, 2023
Accepted: October 19, 2023
Published: October 31, 2023

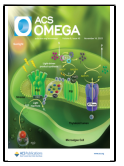

droplets and the possibility of dissolving a substantial amount of CO_2 before injection.

A significant amount of research has been performed on increasing the level of CO_2 adsorption in deep coal seams. One approach is to improve the affinity of coal to adsorb CO_2, which in turn increases its storage capacity. Methyl orange (MO) has been found to modify the coal surface and significantly affect CO_2 molecule charge distribution, increasing CO_2 adsorption.[9] MO modification is found to be feasible only on a laboratory scale and is too complicated for industrial use. Another promising approach is to adapt a surfactant-based method used in the aqueous phase on carbonate rock for enhanced oil recovery. *Glycyrrhiza glabra* has also been studied as a surfactant for flooding on carbonate rock, and the Langmuir adsorption isotherm was found to fit well.[10] However, coal is unlike carbonate rock, which does not have high permeability, and surfactants require higher temperatures to adsorb more effectively. Unfortunately, it is difficult to increase the temperature in underground situations.

Considering the complexity of deep coal seams, this study examined the possibility of sequestering carbon dioxide in shallow coal seams. Due to low confining pressure, CO_2 sequestration in shallow-depth coal seams requires low-pressure injections of gas-phase CO_2.[11] A pilot study conducted in Poland has demonstrated the possibility of CO_2 adsorption at low pressures by using low-rank coal from shallow coal seams, with CO_2 adsorption capacities 30% lower than at high pressures.[12] The adsorption of low-pressure CO_2 on low-rank coal from Poland occurred on multilayers,[11] in contrast to low-rank coal from China, where monolayer adsorption of low-pressure CO_2 was observed.[13] Additionally, coal sample conditions play a significant role in determining CO_2 adsorption capacity. Drying and crushing low-rank coal in Indonesia increase its CO_2 adsorption capacity, with drying having a more significant effect than crushing.[14] Dry coal was also found to have a greater capacity for transporting gases and storing CO_2 than coal containing moisture, while coal with high moisture content had a lower gas adsorption capacity.[15−17] The adsorption capacity of CO_2 is also influenced by other specific characteristics of coal, such as ash yield, maceral content, and coal pore effects.[18−21]

Furthermore, the adsorption of CO_2 on coal is affected by both pressure and temperature. As pressure increases, so does CO_2 adsorption, increasing the permeability and leakage risk.[22−24] On the other hand, increasing gas adsorption capacity decreases.[25] Previous studies have shown that CO_2 injection at pressures lower than 4 MPa and temperatures lower than 323 K can be effective for CO_2 sequestration and ECBM.[26,27] The same pressure and temperature conditions can also illustrate the relationship between CO_2 adsorption and the replaced water mass in natural conditions.[28] Research indicates that low-rank coal from shallow-depth coal seams is more suitable for CO_2 adsorption using pressures lower than 4 MPa and temperatures lower than 323 K. However, it is challenging to recognize the inhibitor factor on CO_2 adsorption at low pressures and temperatures on low-coal rank under different conditions while considering the specific characteristics of coal.

This study aims to investigate the factors inhibiting the binding of CO_2 to low-rank coal surfaces and adsorbing it to micropores and mesopores with low pressure under different conditions. As opposed to another study in which CO_2 adsorption was measured using a coal block to illustrate natural conditions and to simplify the analysis of the inhibitors of CO_2 adsorption on the coal surface until micropore. The adsorption of CO_2 was measured by the volumetric method and fitted to the Langmuir, Freundlich, and Temkin models. Statistical evaluations such as sum square error (SSE) and average relative error (ARE) were used to determine the most suitable adsorption isotherm model. Calculating the experimental data from the Henry coefficients, surface potentials, and Gibbs free energy can determine the affinity, loading, and spontaneous adsorption of CO_2 onto coal. The detection of CO_2 adsorption inhibitors on coal at the meso- and micropore scales was examined using scanning electron microscopy (SEM) and low-temperature nitrogen adsorption (LTNA). A discussion of the inhibitory factors for CO_2 adsorption at shallow depth was presented based on the findings of this study.

2. METHOD

The coal samples were collected from five coal seams (A1, A2, B1, C, and D) in West Banko, South Sumatra Basin, Indonesia (Figure 1). The coal from this area is known to be low-rank coal with significant potential for fuel,[29] rare earth elements,[30] and CO_2 sequestration.[14]

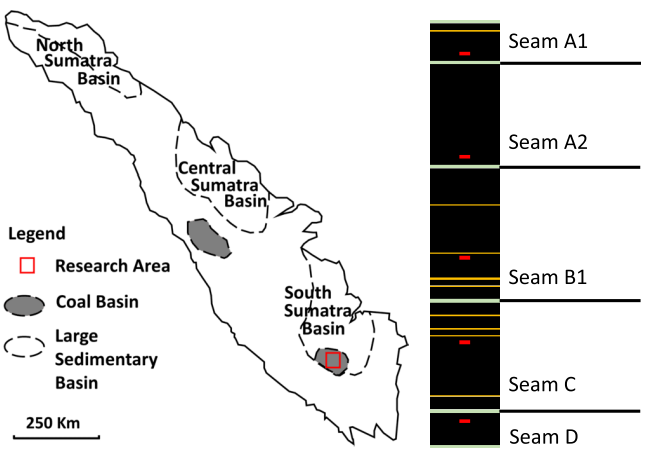

Figure 1. Location of the study area in the South Sumatra Basin, Indonesia. The red box indicates sample locations. The map and coal seam are adapted from the literature.[58]

2.1. Sample Characterization. Table 1 shows the experimental results of proximate analysis samples following ASTM D1373-73, D3174-73, and D3175-77. On the air-received basis, the moisture content of coal samples was relatively high and ranged from 15.18 to 20.11%. The volatile matter (VM) ranged from 49.21 to 55.08%, whereas the ash yield of most coal samples ranged from 1.96 to 2.98%. The fixed carbon content was similar, varying from 44.92 to 50.79%. Seams A1, B1, C, and D showed similar proximate results, but

Table 1. Results of Proximate Analysis of All Coal Seams from the West Banko Area

coal seam	thickness (m)	moisture (%, a.r.)	ash (%, adb)	VM (%, adb)	FC (%, adb)
A1	2.5	17.12	1.96	49.80	50.20
A2	8.6	15.39	2.90	55.08	44.92
B1	10.5	16.48	2.53	49.21	50.79
C	8.5	15.18	2.98	50.29	49.71
D	3.6	20.11	1.97	51.66	48.34

https://doi.org/10.1021/acsomega.3c04615
ACS Omega 2023, 8, 42329−42339

seam A2 showed a higher volatile matter content and a lower fixed carbon content than the other seams.

Table 2 summarizes the experimental results for organic petrography and huminite reflectance (R_o%). For the organic petrography analysis, coal samples were crushed, mounted in polyester resin, polished, and counted under a reflecting light microscope with 550 points. The huminite content ranged from 55.09 to 64.8%, liptinite content varied from 18.95 to 31.09%, inertinite ranged from 10.91 to 18%, and mineral matter ranged from 1.09 to 3.27%. Thermal maturity as a percent of R_o% ranged from 0.37 to 0.50 (average 0.47), which indicates that the coal is of low rank.

Table 2. Experimental Data Results of Organic Petrographic and Reflectance (R_o%)

sample	total huminite (%)	total liptinite (%)	total inertinite (%)	mineral matter (%)	R_o (%)
A1	63.45	23.45	11.09	2.00	0.49
A2	56.18	22.36	18.00	3.27	0.37
B1	64.80	18.95	13.90	2.35	0.50
C	55.09	31.09	10.91	2.91	0.48
D	55.82	27.82	15.27	1.09	0.45

2.2. Coal Conditions for CO_2 Adsorption Isotherms. All the coal samples were shaped into blocks (1 × 1 cm) and prepared in two conditions (raw and dry). Raw coal contained moisture, while dry coal contained no moisture. To conduct an experiment using the coal samples in dry conditions, samples were dried in a vacuum furnace until their weights remained constant. After the coal samples were dried, they were immediately transferred to the sample cell to avoid oxidation or moisture contamination. In this study, a block shape was selected to represent the natural state of coal.

2.3. CO_2 Adsorption Isotherm Experiment. This study used an adsorption apparatus constructed from fabricated materials. The setup consisted of two fixed-volume cells, one for the reference cell and the other for the sample cell (Figure 2). The CO_2 adsorption experiment began by opening the intake flow valve to let the CO_2 enter the referenced cell. After reaching the desired pressure, it was monitored for 30 min or until it remained unchanged. By opening the connecting valve, CO_2 was allowed to enter the sample cell and adsorb onto the coal block sample. An equilibrium state was achieved after monitoring the pressure in reference and sample cells for 6 to 24 h or remaining constant. By opening the exhaust flow valve and using a vacuum pump, CO_2 was allowed to exit the system.

2.4. CO_2 Adsorption Experiment. To determine the adsorption of CO_2 onto the coal sample, we constructed a volumetric adsorption apparatus. The experiment pressure was set up to 3 MPa at 318.15 K. The experiment data of CO_2 adsorption can be calculated by the following equation[25]

$$\Delta n^{ex} = \left(\frac{1}{RTm}\right)\left(V_{rc}\left(\frac{P_{rci}}{Z_{rci}} - \frac{P_{rcf}}{Z_{rcf}}\right) - V_{void}\left(\frac{P_{scf}}{Z_{scf}} - \frac{P_{sci}}{Z_{sci}}\right)\right) \quad (1)$$

where Δn^{ex} is the amount of excess adsorption (mmol g^{-1}); R is the molar gas constant (8.314 J mol^{-1} K^{-1}); T is the temperature (K); m is the mass of coal (g); V_{rc} is the reference cell (cm^3); V_{void} is the void volume (cm^3); P_{rci} is the initial pressure of reference cells (MPa); P_{rcf} is the final pressure of reference cells (MPa); P_{sci} is the initial pressure of sample cells (MPa); Z_{rci} is the reference cell initial compressibility factor; Z_{rcf} is the reference cell final compressibility factor; Z_{sci} is the sample cell initial compressibility factor; and Z_{scf} is the sample cell final compressibility factor.

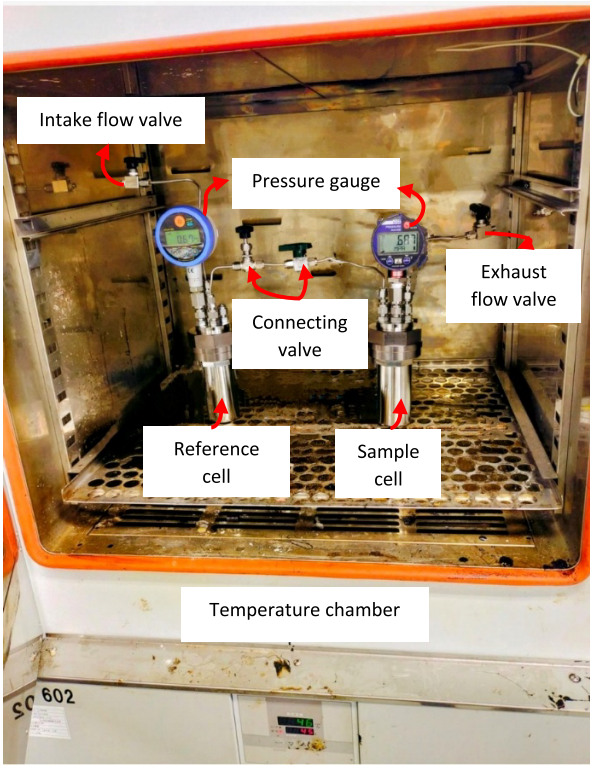

Figure 2. Volumetric method for CO_2 adsorption on coal.

The Z value in eq 1 is given by eq 2. In eq 2, P_r and T_r can be solved by eqs 3 and 4.[25]

$$Z = 1 + \left(0.083 - \frac{0.422}{T_r^{1.6}}\right)\frac{P_r}{T_r} + \omega\left(0.139 - \frac{0.172}{T_r^{4.2}}\right)\frac{P_r}{T_r} \quad (2)$$

$$P_r = \frac{P}{P_c} \quad (3)$$

$$T_r = \frac{T}{T_c} \quad (4)$$

where P is the pressure on the experiment (MPa); P_r is the reduced pressure; T_r is the reduced temperature; ω is the acentric factor (CO_2 is 0.224); P_c is the critical pressure (CO_2 is 7.39 MPa); and T_c is the critical temperature (CO_2 is 304.2 K).

2.5. CO_2 Adsorption Isotherm Models. The process of adsorbing pure CO_2 was simulated using adsorption isotherm models to verify the adsorption. The two-parameter isotherm constants can be determined through linear regression by transforming the isotherm variables into a linear form.[31,32] There are two isotherm models used to fit the experimental data of the CO_2 adsorption onto the coal: the Langmuir isotherm model identifies CO_2 adsorption on the monolayers of coal, while the Freundlich and Temkin isotherm model identifies CO_2 adsorption on the multilayers of coal.[33−35] Between Freundlich and Temkin isotherm models, Temkin is more sensitive to the changes for the CO_2 adsorption on coal surfaces.

https://doi.org/10.1021/acsomega.3c04615
ACS Omega 2023, 8, 42329−42339

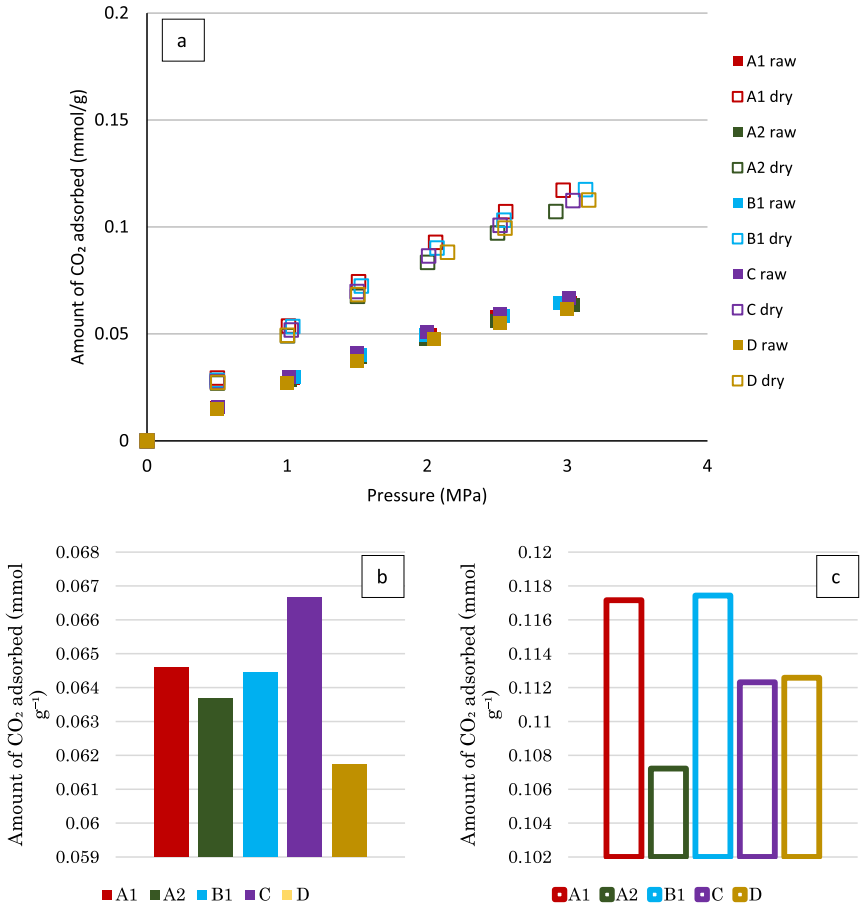

Figure 3. (a) Experimental data of CO_2 adsorption on coal and detailed CO_2 adsorption on 3 MPa (b) under raw conditions and (c) under dry conditions.

In the Langmuir isotherm model, the CO_2 adsorption calculation is given by[36]

$$Q_{eL} = \frac{V_L P}{P_L + P} \tag{5}$$

where Q_{eL} is the Langmuir isotherm model adsorbed-gas storage capacity ($cm^3\ g^{-1}$); P is the pressure on the experiment (MPa); V_L is the Langmuir volume ($cm^3\ g^{-1}$); and P_L is the Langmuir pressure (MPa).

In the Freundlich's isotherm model, CO_2 adsorption can be calculated as follows[37]

$$Q_{eF} = K_f P_{CO_2}^{\ 1/n} \tag{6}$$

where Q_{eF} is the Freundlich isotherm model adsorbed-gas storage capacity ($cm^3\ g^{-1}$); P_{CO_2} is the pressure when CO_2 is injected (MPa); K_f is the Freundlich constant; and n is the heterogeneity factor.

According to the Temkin adsorption isotherm model, the amount of adsorbed CO_2 can be calculated as follows[38]

$$q_{eT} = \frac{RT}{b_T} \ln(K_T P) \tag{7}$$

where q_{eT} is the volume of gas adsorbed based on the Temkin isotherm model ($cm^3\ g^{-1}$); b_T is the Temkin isotherm constant; P is the pressure on the experiment (MPa), and K_T is the Temkin constant.

2.6. Statistical Evaluation of the Adsorption Isotherm Model. Much research has utilized standard models, such as Langmuir, Freundlich, and Temkin, to obtain liquid−solid and gas−solid adsorption data. The validity of these models is frequently evaluated experimentally based on their ability to match the data and their coherency with physicochemical data.[39] Data analysis methods such as sum square error (SSE) and average relative error (ARE) were employed to determine the statistical goodness-of-fit. SSE is the most commonly used method for liquid-phase concentrations since this method more accurately fits the isotherm.[40] SSE was calculated by[41]

$$\mathrm{SSE} = \sum_{i=1}^{n} (q_{\mathrm{model}} - q_{\mathrm{experimental\ data}})_i^2 \tag{8}$$

The ARE model tends to underestimate or overestimate the experimental data to minimize the fractional error distribution across the entire concentration ranges.[42] This method is applied by[41]

$$\mathrm{ARE} = \frac{100}{n} \sum_{i=1}^{n} \left| \frac{q_{\mathrm{model}} - q_{\mathrm{experimental\ data}}}{q_{\mathrm{experimental\ data}}} \right|_i \tag{9}$$

where i is the initial condition and n is the number of data points.

2.7. Affinity and Spontaneous Adsorption of CO_2. Henry's coefficient surface potential and Gibbs free energy were examined to understand CO_2 adsorption. The Henry coefficient (K_H) measures the affinity of adsorbed molecules for porous

https://doi.org/10.1021/acsomega.3c04615
ACS Omega 2023, 8, 42329−42339

Table 3. CO_2 Adsorption Isotherm Model of All Coal Seams from the West Banko Area

		isotherm model								
		Langmuir			Freundlich			Temkin		
coal seam	coal condition	V_L	P_L	R^2	n	K	R^2	BT	KT	R^2
A1	raw	0.18	5.27	0.9997	0.80	0.03	0.9983	0.03	3.13	0.9816
	dry	0.30	4.65	0.9995	0.78	0.05	0.9989	0.05	3.24	0.9797
A2	raw	0.18	5.31	0.9759	0.80	0.03	0.9984	0.03	3.12	0.9793
	dry	0.28	4.73	0.9991	0.79	0.05	0.9988	0.05	3.23	0.9767
B1	raw	0.18	5.27	0.9942	0.80	0.03	0.9987	0.03	3.14	0.9796
	dry	0.29	4.66	0.9986	0.78	0.05	0.9985	0.05	3.21	0.9778
C	raw	0.18	5.26	0.9999	0.80	0.03	0.9985	0.03	3.13	0.9805
	dry	0.29	4.67	1.0000	0.72	0.05	0.9261	0.05	3.23	0.9797
D	raw	0.17	5.32	0.9996	0.80	0.03	0.9983	0.03	3.11	0.9806
	dry	0.28	4.69	0.9993	0.78	0.05	0.9983	0.05	3.18	0.9757

media surfaces, where adsorption affinity increases with increasing Henry coefficient.[34] The relationship between equilibrium pressure (P) and adsorption quantity (q) can be expressed using the virial equation expressed as[43]

$$\frac{P}{q} = \frac{1}{K_H}\exp(A_1 q + \ldots) \tag{10}$$

The K_H value at low pressure can be calculated by fitting the linear region $\ln(P/q)$ versus the amount of adsorption (q).[44]

$$\ln(P/q) = A_0 + A_1 q \tag{11}$$

where the value of K_H corresponds to A_0 since $K_H = \exp(-A_0)$.

The thermodynamics of adsorption contributes to understanding the mechanism of spontaneous adsorption.[45] In particular, this study examines the surface potential (Ω) and Gibbs free energy (ΔG). An estimate of the energy released from the adsorbate attached to the adsorbent surface is given by[26]

$$\Omega = -RT\int_0^P \frac{V}{P}\mathrm{d}P \tag{12}$$

As an indicator of reaction spontaneity, the Gibbs free energy is calculated as follows.[26]

$$\Delta G = \frac{\Omega}{V} \tag{13}$$

2.8. CO_2 Adsorption on the Coal Pore. Coal pores can be classified into three main types according to the International Union of Pure and Applied Chemistry (IUPAC): macropores (≥50 nm in diameter); mesopores or transitional pores (2−50 nm in diameter); nanometers in diameter); mesopores (2−4 nm in diameter); and micropores (≤2 nm in diameter).[46] This study used SEM images, and low-pressure N_2 adsorption at 77 K was used to examine coal pores and inhibit pore connectivity.

3. RESULTS AND DISCUSSION

3.1. Experimental and Isothermal Analysis of CO_2 Adsorption. Experimental data indicate that the CO_2 adsorption capacity increases with pressure (Figure 3a). Adsorption on coal shows similarity between pressures of 0.5 to 2 MPa but is more varied at higher pressures (2−3 MPa). It is worth noting that the volumetric method for measuring CO_2 adsorption has an equilibrium state accuracy of ±0.003. When the pressure is low, the slight difference in the equilibrium pressure before and after adsorption can lead to a higher chance of experimental error.

CO_2 adsorption experiments on raw coal revealed that C coal seams had better CO_2 adsorption capacity than other coal seams due to the lower moisture content (Figure 3b). Experimental data on CO_2 adsorption on dry coal showed that the B1 coal seam resulted in higher CO_2 adsorption capacity than the other coal seams due to higher fixed carbon content (Figure 3c). The comparison of the CO_2 adsorption capacity between raw and dry conditions at 3 MPa showed that the drying process increased the CO_2 adsorption capacity by 1.6−1.8 times (Figure 3). Lower CO_2 adsorption capacity in raw coal was observed due to the presence of water molecules in the pores and surfaces of the coal, making it difficult for CO_2 to adsorb to the pores and surfaces of coal.[47] Dry conditions are more favorable for CO_2 adsorption due to the absence of water molecules in the coal surface and pores, resulting in more accessible sites for adsorption.

The fitting graph between the experimental data, the adsorption isotherm model, and the detailed parameters is shown in Table 3. According to the fitting graph, CO_2 adsorption occurs similarly in raw and dry conditions (Figure 4). All adsorption isotherm models tended to match the

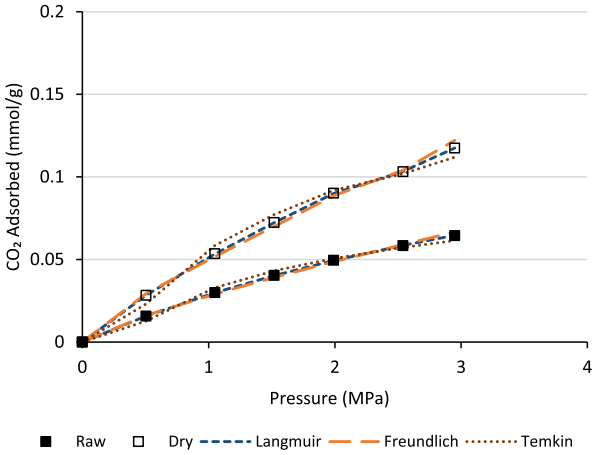

Figure 4. Langmuir, Freundlich, and Temkin isotherm models fit CO_2 adsorption on the B coal seam in raw or dry conditions for the block.

experimental data well, as the coefficient of determination (R^2) was more than 0.97. Langmuir and Freundlich adsorption models were better fitted than Temkin's adsorption model based on the coefficient of determination between an adsorption isotherm model and the CO_2 adsorption experiments.

Langmuir proved to be the superior option compared with Freundlich, especially at higher pressures (Figure 4). The

https://doi.org/10.1021/acsomega.3c04615
ACS Omega 2023, 8, 42329−42339

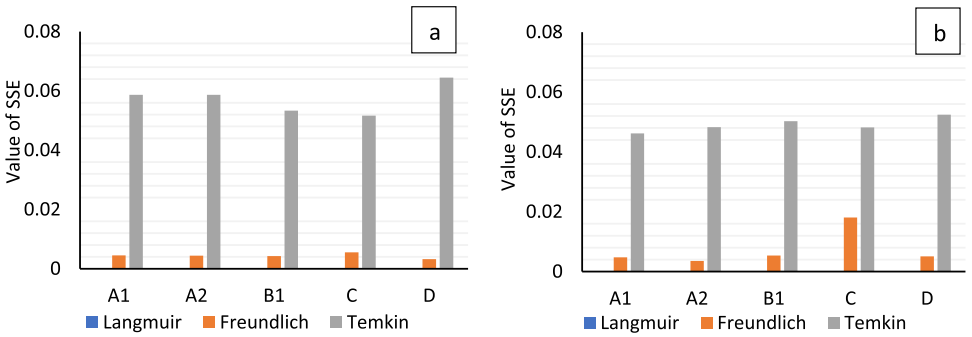

Figure 5. Value of SSE of isotherm models (a) under the raw condition and (b) under the dry condition.

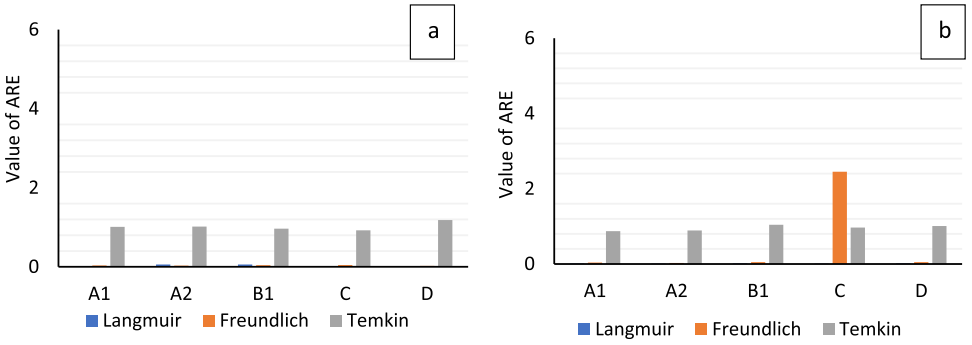

Figure 6. Value of ARE of isotherm models (a) under the raw condition and (b) under the dry condition.

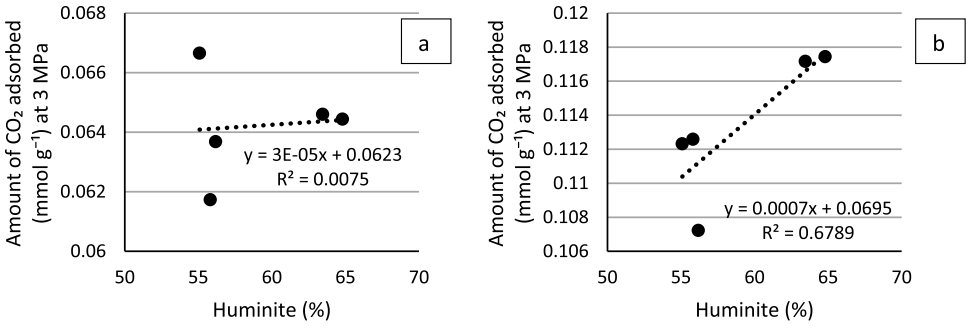

Figure 7. Relationship between CO_2 adsorption and huminite content in the (a) raw condition and (b) dry condition.

Langmuir model provided a better fit, making it the more reliable choice for accurate and precise data analysis. To address the unreliability issue in the Freundlich adsorption isotherm model for high-pressure data,[31] this study used low-pressure and fitted the experimental data with the Freundlich model. It was shown that the goodness of fit with the Freundlich isotherm model widened with increasing pressure (up to 2.5 MPa). Therefore, the Freundlich isotherm model may fit better at low pressures than at higher pressures.

Fitting of experimental data with adsorption isothermal models indicates that CO_2 adsorption at low pressure occurs in monolayers and multilayers. Based on the experimental data obtained in this study, the Temkin adsorption isotherm model was considered unsuitable. The Temkin equation is suitable for describing multilayer adsorption experiments[38] but inadequate for describing pure CO_2 adsorption experiments.[31]

3.2. Statistical Evaluation. The most appropriate isothermal model was determined using a combination of coefficients of determination and error functions such as SSE and ARE. The Langmuir isotherm model had the lowest SSE value, whereas the Temkin isotherm model had the highest (Figure 5). The Langmuir and Freundlich adsorption isotherm models better fit the experimental data, indicating that low-pressure CO_2 adsorption can occur in monolayers and multilayers. SSE analysis revealed similar results regardless of whether the coal samples were raw or dry. The Temkin isotherm model appeared to have the most significant average relative error under raw and dry conditions (Figure 6). In the case of anomalous values, another isotherm model (such as Langmuir or Freundlich) is probably more appropriate.

3.3. Relation between CO_2 Adsorption and Organic Composition. Coal contains organic constituents known as macerals and can be further classified into huminite, liptinite, and inertinite. The correlation between CO_2 adsorption and maceral content varies depending on the maceral content. There was a positive correlation between CO_2 adsorption and huminite content in raw and dry conditions (Figure 7). Huminite provides a favorable environment for CO_2 adsorption,[48] possibly due to the maceral-containing micropore connection,[49] that facilitates gas transport into micropores. It is known that huminite contains more oxygen functional groups than other macerals, where oxygen-containing functional groups

https://doi.org/10.1021/acsomega.3c04615
ACS Omega 2023, 8, 42329−42339

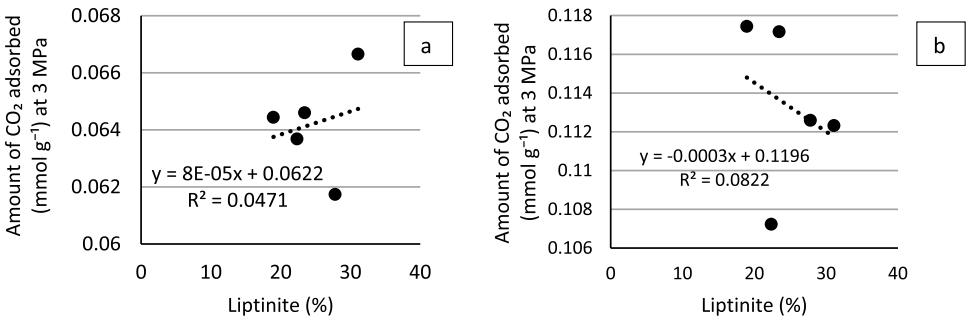

Figure 8. Relationship between CO_2 adsorption and liptinite content in the (a) raw condition and (b) dry condition.

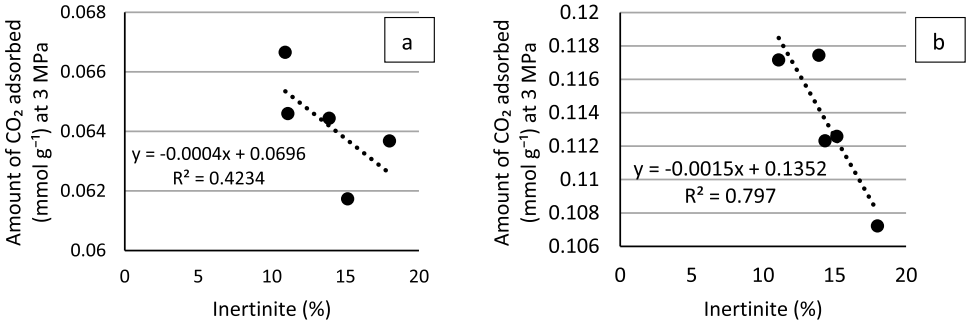

Figure 9. Relationship between CO_2 adsorption and inertinite content in the (a) raw condition and (b) dry condition.

related to active sites positively affect CO_2 adsorption on coal.[23,50,51] Furthermore, the fitted results of CO_2 adsorption onto dry coal with huminite content indicate that the drying process enhances the positive correlation between the CO_2 adsorption and huminite content.

Figure 8 illustrates the relationship between the CO_2 adsorption and liptinite in this study. Based on the fitting of the CO_2 adsorption with liptinite, it was apparent that the adsorption of CO_2 has a positive correlation in the raw condition but not in the dry condition. This different correlation between the raw and dry conditions indicated that liptinite has a weakly positive correlation with CO_2 adsorption.

In contrast to huminite and liptinite, inertinite is highly effective in inhibiting CO_2 adsorption[52] (Figure 9). According to the surface properties of inertinite, it is less hydrophobic than huminite, which makes it difficult for water to drain since inertinite is more porous than huminite, and it interacts more strongly with water than with huminite.[53] Moreover, inertinite has a higher concentration of aromatic compounds and a more condensed structure with fewer reactive groups than other macerals.[50,54]

3.4. Henry Coefficient, Surface Potentials, and Gibbs Free Energy of CO_2 on Coals. Figure 10 illustrates Henry coefficients (K_H) for the adsorption of CO_2 on coal samples under different conditions. The result shows that the difference in K_H values between the raw and dry conditions for all coal seams is significant where the drying process increases K_H values by 80−100%. The higher K_H value in dry coal increases the affinity between coal molecules and CO_2 due to a significant decrease in moisture during the drying process.[45,55] Coal seam C had the highest K_H values under raw conditions compared to those of the other coal seams. As seam C has the lowest moisture content and high levels of huminite and liptinite, it has more potential for adsorbing CO_2. Although seam A2 has a lower moisture content than coal seams A1, B1, and D, it has a high huminite content, which inhibits CO_2 adsorption and results in a

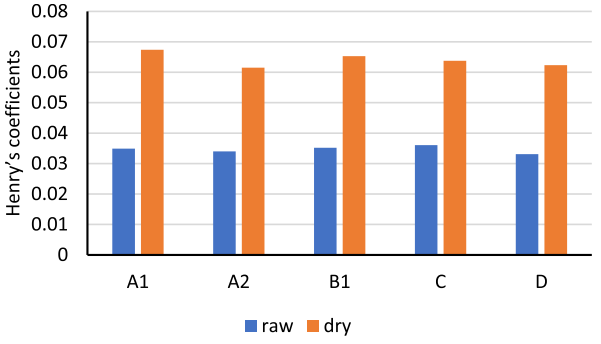

Figure 10. Henry's coefficients of CO_2 on raw and dry conditions.

lower K_H value than coal seam A1, B1, C, and D. Under dry conditions, coal seam B1 had the highest K_H values. This condition is due to coal seam B1 having the highest huminite content than other coal seams, which shows that the absence of water molecule on coal increases the binding of CO_2 adsorption with coal. According to the current study, the inhibited interaction between coal and CO_2 was affected not only by the moisture content but also by the maceral content, such as inertinite.

The graph of surface potential indicates that when the pressure reaches zero, the Ω value approaches zero, while when the pressure increases, the Ω values exhibit negative values (Figure 11). High pressure requires significant isothermal work to load the adsorbate molecules into the pores, which increases Ω. The value of Ω in dry coal was higher than that in raw coal due to the drying process, making the coal sites more accessible for CO_2 adsorption. This study found a similar Ω value in raw coal, with coal seams C and B1 having a slightly higher value than the other coal seams. The seams A1, B1, and C show a high value of Ω in dry conditions. However, seam A1 does not qualify as a candidate for CO_2 storage in the raw condition since seam A1 had higher moisture content than seams B1 and C.

https://doi.org/10.1021/acsomega.3c04615
ACS Omega 2023, 8, 42329−42339

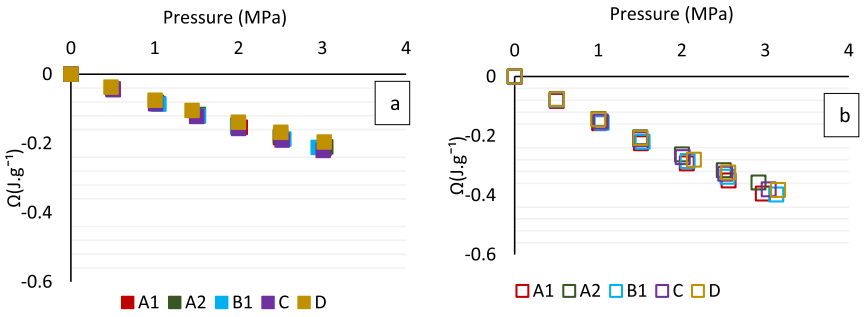

Figure 11. Surface potentials of CO_2 under different conditions: (a) raw and (b) dry.

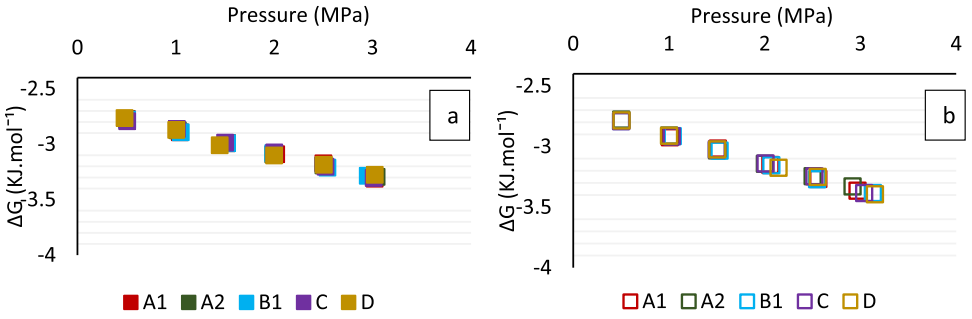

Figure 12. Gibbs free energy of CO_2 under four different conditions: (a) block-raw and (b) block-dry.

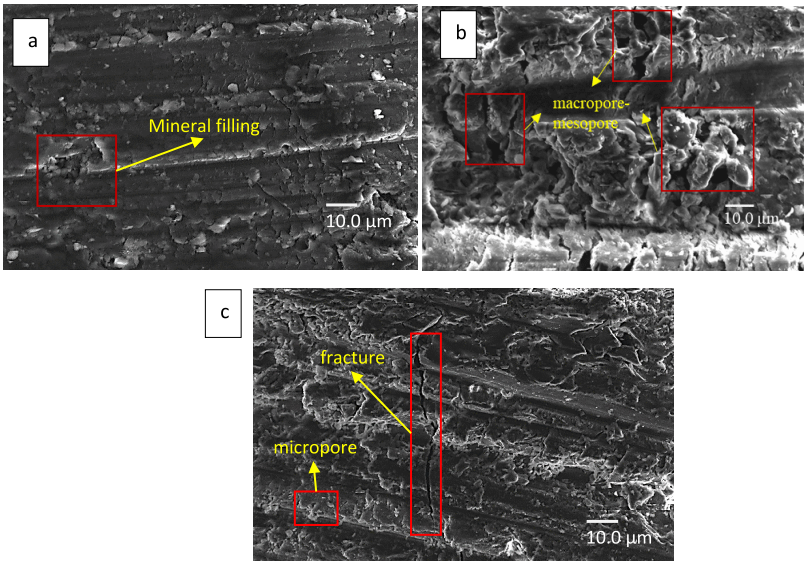

Figure 13. SEM image of different conditions: (a) raw condition, (b) raw condition after CO_2 adsorption, and (c) dry condition after CO_2 adsorption.

Additionally, seam A1 had high huminite content where moisture content decreases due to the drying process, resulting in increasing potential to adsorb CO_2. On the other hand, seam A2 was considered incapable of storing CO_2 in dry conditions since it contained high levels of inertinite.

The graph of Gibbs free energy showed a negative value in which an increase in the CO_2 pressure led to a rise in the ΔG for CO_2 (Figure 12). The high moisture content in coal seams, such as seams A1 and D, had more positive ΔG values than other coal seams, indicating that moisture weakens the spontaneous adsorption process of CO_2. CO_2 adsorption occurred more spontaneously on seams B1 and C, similar to the Henry coefficient and surface potential for the adsorption of CO_2 on raw coal. However, under dry conditions, seam D could potentially adsorb CO_2. Since seam D had a high moisture content, drying the seam increased the coal's spontaneity to adsorb CO_2. Experimental data on CO_2 adsorption onto dry coal showed that seams A1, B1, C, and D exhibited similar ΔG values with rising pressure, leading to an increase in ΔG value. In contrast, seam A2 demonstrated that increasing the pressure did not increase spontaneous CO_2 adsorption.

3.5. Inhibition of CO_2 Adsorption on Coal Pores. In the raw condition, pores were generally oval and filled with minerals (Figure 13a). Observation of raw coal after CO_2 injection showed that raw coal was dominated by macropores and micropores, with some pores not filled with minerals (Figure 13b). CO_2 entered the coal body and created an acidic environment, causing minerals to dissolve (Wang and co-workers). Future research needs to address further the effect of pore opening caused by mineral leaching on the adsorption of

https://doi.org/10.1021/acsomega.3c04615
ACS Omega 2023, 8, 42329−42339

CO_2. SEM can detect shrinkage traces generated by the drying process (Figure 13c) as shrinkage occurs from coal structure disruption due to moisture removal.[56]

This study used LTNA to detect micropore size changes. LTNA results showed peaks of micropores in raw coal ranging from 0.7 to 1.1 nm and from 1.8 to 1.9 nm. However, micropores were absent after the adsorption of CO_2 onto the raw coal (Figure 14). The differences observed between raw coal before and after CO_2 adsorption may be attributed to the process of CO_2 adsorption. Injection of CO_2 leads to elimination of micropores in raw coal, causing swelling that results in the closing of micropores and reduced pore access. The observed differences may also be due to the effect of coal compressibility.[57] In coal, moisture changes may contribute to pore size changes.[52] In this study, CO_2 adsorption onto raw and dry coal revealed differences in the micropores that might still exist in the dry coal case. The graph illustrates the peak micropore size being 1.5−1.7 nm. Based on these results, moisture loss opens up more sites and micropores for CO_2 adsorption. Although CO_2 adsorption can lead to swelling in raw coal, the swelling does not close all of the micropores in dry coal.

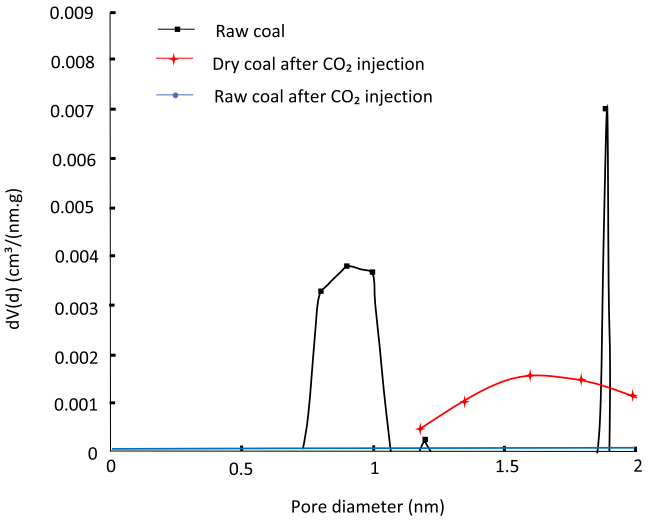

Figure 14. Micropore size distribution of coal samples before and after CO_2 injection under different conditions.

CO_2 adsorption on low-rank coal from shallow-depth coal seams shows that the moisture and inertinite contents significantly inhibit CO_2 adsorption. Moreover, minerals have the potential to inhibit the adsorption of CO_2 in coal. Upon removal of the minerals, the amount of CO_2 adsorption can be maximized. To better understand the effects of leaching on minerals during the adsorption of CO_2 onto the coal, it is necessary to conduct further research.

According to the research, the inhibitory factor of the adsorption of CO_2 on low-rank coal at shallow-depth coal seams can be used to determine the suitability of a coal seam for CO_2 sequestration. The coal seams with lower moisture levels and a lower percentage of inertinite are considered the best options for the CO_2 sequestration. However, it is essential to note that this study has some limitations. This study considers CO_2 adsorption on coal under dry conditions, which does not represent in situ conditions since it can be challenging to dry low-rank coal in natural settings to full potential. Additionally, coal properties vary from one area to another, making it challenging to apply the findings of this research to other regions directly.

4. CONCLUSIONS

The study of inhibitory factors of CO_2 adsorption on five coal seams in South Sumatra led to the following conclusions: in CO_2 adsorption experiments, it has been shown that moisture inhibits CO_2 adsorption on coal, with the CO_2 adsorption capacity of dry coal, which is 1.6−1.8 times higher than that of raw coal. The statistical evaluation showed that CO_2 adsorption on low-rank coal under low pressure resulted in affinity for monolayers and multilayers. In the petrographic analysis, coal with high inertinite had the lowest CO_2 adsorption experimentally, and coal conditions did not affect CO_2 adsorption inhibition by inertinite. The presence of moisture and inertinite also inhibited CO_2 affinity, accommodation, and spontaneous CO_2 adsorption on coal. CO_2 adsorption experiments have shown that CO_2 can adsorb into coal micropores, with a marked change in the micropore size. There was more than one peak in the micropores in raw coal and no micropore peak after the CO_2 adsorption. It is possible that mineral leaching could open the closed pores, increasing the possibility of the adsorption of CO_2 on coal. However, this requires additional research. The results of CO_2 adsorption at low pressure were similar for different coal seams in the same area from shallow depths. However, coal seam D with high moisture showed lower CO_2 adsorption in the raw condition compared to that of other coal seams, and coal seam A2 with high inertinite showed lower CO_2 adsorption. Although similar results were obtained in this study, understanding the inhibitor factors will allow the identification of potential coal seams. According to this study, coal seams B1 and C may be capable of adsorbing CO_2.

Further research can be conducted to address the limitations and findings of this study. For instance, future studies can investigate the safety and efficacy of CO_2 adsorption in reducing the moisture content. Additionally, future research can explore the correlation between the aromatic group in maceral found in South Sumatra low-rank coal and the CO_2 adsorption.

AUTHOR INFORMATION

Corresponding Author

Theodora Noely Tambaria − *Department of Earth Resources Engineering, Kyushu University, Nishiku, Fukuoka 819-0395, Japan*; orcid.org/0000-0002-7087-0568; Email: tambaria.noely.theodora.921@m.kyushu-u.ac.jp

Authors

Yuichi Sugai − *Department of Earth Resources Engineering, Kyushu University, Nishiku, Fukuoka 819-0395, Japan*

Ferian Anggara − *Department of Geological Engineering, Faculty of Engineering and Unconventional Geo-Resources Research Group, Faculty of Engineering, Universitas Gadjah Mada, Yogyakarta, Daerah Istimewa Yogyakarta 55281, Indonesia*

Complete contact information is available at: https://pubs.acs.org/10.1021/acsomega.3c04615

Notes

The authors declare no competing financial interest.

https://doi.org/10.1021/acsomega.3c04615
ACS Omega 2023, 8, 42329−42339

■ ACKNOWLEDGMENTS

The authors thank PT Bukit Asam and the Unconventional Geo-Resources Research Group, Faculty of Engineering, Universitas Gadjah Mada, for providing the coal samples.

■ REFERENCES

(1) Shimada, S.; Li, H.; Oshima, Y.; Adachi, K. Displacement Behavior of CH4 Adsorbed on Coals by Injecting Pure CO2, N2, and CO2-N2Mixture. *Environ. Geol.* **2005**, *49* (1), 44−52.

(2) Oudinot, A. Y.; Riestenberg, D. E.; Koperna, G. J. Enhanced Gas Recovery and CO2 Storage in Coal Bed Methane Reservoirs with N2 Co-Injection. *Energy Procedia* **2017**, *114*, 5356−5376. November 2016

(3) Gale, J.; Freund, P. Coal-Bed Methane Enhancement with CO2 Sequestration Worldwide Potential. *Environ. Geosci.* **2001**, *8* (3), 210−217.

(4) Saghafi, A.; Faiz, M.; Roberts, D. CO2 Storage and Gas Diffusivity Properties of Coals from Sydney Basin, Australia. *Int. J. Coal Geol* **2007**, *70*, 240−254.

(5) Kolak, J. J.; Burruss, R. C. *A Geochemical Investigation into the Effect of Coal Rank on the Potential Environmental Effects of CO 2 Sequestration in Deep Coal Beds U. S. Department of the Interior*; 2004. 1−3 SPEC. ISS.

(6) Xie, H. P.; Zhou, H. W.; Xue, D. J.; Wang, H. W.; Zhang, R.; Gao, F. Research and Consideration on Deep Coal Mining and Critical Mining Depth. *Meitan Xuebao/J. China Coal Soc.* **2012**, *37* (4), 535−542.

(7) Zhou, Y.; Li, Z.; Zhang, R.; Wang, G.; Yu, H.; Sun, G.; Chen, L. CO2 Injection in Coal: Advantages and Influences of Temperature and Pressure. *Fuel* **2019**, *236*, 493−500. September 2018

(8) Zendehboudi, S.; Khan, A.; Carlisle, S.; Leonenko, Y. Ex Situ Dissolution of CO2: A New Engineering Methodology Based on Mass-Transfer Perspective for Enhancement of CO2 Sequestration. *Energy Fuels* **2011**, *25* (7), 3323−3333.

(9) Abid, H. R.; Iglauer, S.; Al-Yaseri, A.; Keshavarz, A. Drastic Enhancement of CO2 Adsorption Capacity by Negatively Charged Sub-Bituminous Coal. *Energy* **2021**, *233*, No. 120924.

(10) Ahmadi, M. A.; Zendehboudi, S.; Shafiei, A.; James, L. Nonionic Surfactant for Enhanced Oil Recovery from Carbonates: Adsorption Kinetics and Equilibrium. *Ind. Eng. Chem. Res.* **2012**, *51* (29), 9894−9905.

(11) Sadasivam, S.; Masum, S.; Chen, M.; Stańczyk, K.; Thomas, H. Kinetics of Gas Phase CO2Adsorption on Bituminous Coal from a Shallow Coal Seam. *Energy Fuels* **2022**, *36* (15), 8360−8370.

(12) Masum, S. A.; Sadasivam, S.; Chen, M.; Thomas, H. R. Low Subcritical CO2 Adsorption-Desorption Behavior of Intact Bituminous Coal Cores Extracted from a Shallow Coal Seam. *Langmuir* **2023**, *39* (4), 1548−1561.

(13) Guo, H.; Cheng, Y.; Wang, L.; Lu, S.; Jin, K. Experimental Study on the Effect of Moisture on Low-Rank Coal Adsorption Characteristics. *J. Nat. Gas Sci. Eng.* **2015**, *24*, 245−251.

(14) Tambaria, T. N.; Sugai, Y.; Anggara, F. Experimental Measurements of CO2 Adsorption on Indonesian Low-Rank Coals under Various Conditions. *J. Pet. Explor. Prod. Technol.* **2023**, *13* (3), 813−826.

(15) Zheng, S.; Yao, Y.; Elsworth, D.; Liu, D.; Cai, Y. Dynamic Fluid Interactions during CO2-ECBM and CO2 Sequestration in Coal Seams. Part 2: CO2-H2O Wettability. *Fuel* **2020**, *279*, No. 118560.

(16) Crosdale, P. J.; Moore, T. A.; Mares, T. E. Influence of Moisture Content and Temperature on Methane Adsorption Isotherm Analysis for Coals from a Low-Rank, Biogenically-Sourced Gas Reservoir. *Int. J. Coal Geol.* **2008**, *76* (1−2), 166−174.

(17) Krooss, B. M.; Van Bergen, F.; Gensterblum, Y.; Siemons, N.; Pagnier, H. J. M.; David, P. High-Pressure Methane and Carbon Dioxide Adsorption on Dry and Moisture-Equilibrated Pennsylvanian Coals. *Int. J. Coal Geol.* **2002**, *51* (2), 69−92.

(18) Li, X.; Fu, X.; Liu, A.; An, H.; Wang, G.; Yang, X.; Wang, L.; Wang, H. Methane Adsorption Characteristics and Adsorbed Gas Content of Low-Rank Coal in China. *Energy Fuels* **2016**, *30* (5), 3840−3848.

(19) Kiani, A.; Sakurovs, R.; Grigore, M.; Sokolova, A. Gas Sorption Capacity, Gas Sorption Rates and Nanoporosity in Coals. *Int. J. Coal Geol.* **2018**, *200*, 77−86.

(20) Maphala, T.; Wagner, N. J. Effects of CO2 Storage in Coal on Coal Properties. *Energy Procedia* **2012**, *23*, 426−438.

(21) Tambaria, T. N.; Sugai, Y.; Nguele, R. Adsorption Factors in Enhanced Coal Bed Methane Recovery: A Review. *Gases* **2022**, *2* (1), 1−21.

(22) Zhu, C.; Wan, J.; Tokunaga, T. K.; Liu, N.; Lin, B.; Wu, H. Impact of CO2 Injection on Wettability of Coal at Elevated Pressure and Temperature. *Int. J. Greenh. Gas Control* **2019**, *91*, No. 102840.

(23) Wang, Q.; Li, W.; Zhang, D.; Wang, H.; Jiang, W.; Zhu, L.; Tao, J.; Huo, P.; Zhang, J. Influence of High-Pressure CO2 Exposure on Adsorption Kinetics of Methane and CO2 on Coals. *J. Nat. Gas Sci. Eng.* **2016**, *34*, 811−822.

(24) Masum, S. A.; Chen, M.; Hosking, L. J.; Stanczyk, K.; Kapusta, K.; Thomas, R. International Journal of Greenhouse Gas Control A Numerical Modelling Study to Support Design of an In-Situ CO 2 Injection Test Facility Using Horizontal Injection Well in a Shallow-Depth Coal Seam. *Int. J. Greenh. Gas Control* **2022**, *119*, 388. July

(25) Abunowara, M.; Sufian, S.; Bustam, M. A.; Eldemerdash, U.; Suleman, H.; Bencini, R.; Assiri, M. A.; Ullah, S.; Al-Sehemi, A. G. Experimental Measurements of Carbon Dioxide, Methane and Nitrogen High-Pressure Adsorption Properties onto Malaysian Coals under Various Conditions. *Energy* **2020**, *210*, No. 118575.

(26) Hao, M.; Qiao, Z.; Zhang, H.; Wang, Y.; Li, Y. Thermodynamic Analysis of CH4/CO2/N2Adsorption on Anthracite Coal: Investigated by Molecular Simulation. *Energy Fuels* **2021**, *35* (5), 4246−4257.

(27) Wen, H.; Hao, J.; Ma, L.; Zheng, X. Experimental Study on Replacing Coal Seam CH4with CO2Gas. *ACS Omega* **2022**, *7* (1), 1395−1403.

(28) Sun, X.; Yao, Y.; Liu, D.; Elsworth, D.; Pan, Z. Interactions and Exchange of CO2 and H2O in Coals: An Investigation by Low-Field NMR Relaxation. *Sci. Rep.* **2016**, *6*, 1−11. January

(29) Waluyo, B. H. *The Assessment of Banko Barat Coal of South Sumatra as a Fuel for the Suralaya Steam Power Electric Generating Plant in West of Java, Indonesia*; 1992.

(30) Anggara, F.; Amijaya, D. H.; Harijoko, A.; Tambaria, T. N.; Sahri, A. A.; Asa, Z. A. N. Rare Earth Element and Yttrium Content of Coal in the Banko Coalfield, South Sumatra Basin, Indonesia: Contributions from Tonstein Layers. *Int. J. Coal Geol.* **2018**, *196*, 159−172.

(31) Mabuza, M.; Premlall, K.; Daramola, M. O. Modelling and Thermodynamic Properties of Pure CO2 and Flue Gas Sorption Data on South African Coals Using Langmuir, Freundlich, Temkin, and Extended Langmuir Isotherm Models. *Int. J. Coal Sci. Technol.* **2022**, *9*, 45.

(32) Ho, Y. S.; Porter, J. F.; Mckay, G. Divalent Metal Ions Onto Peat: Copper, Nickel and Lead Single Component Systems. *Water, Air, Soil Pollut.* **2002**, *141* (1−4), 1−33.

(33) Adams, J. J. Asphaltene Adsorption, a Literature Review. *Energy Fuels* **2014**, *28* (5), 2831−2856.

(34) Montoya, T.; Coral, D.; Franco, C. A.; Nassar, N. N.; Cortés, F. B. A Novel Solid-Liquid Equilibrium Model for Describing the Adsorption of Associating Asphaltene Molecules onto Solid Surfaces Based on the "Chemical Theory. *Energy Fuels* **2014**, *28* (8), 4963−4975.

(35) Mahmoud, M.; Eliebid, M.; Al-Yousef, H. Y.; Kamal, M. S.; Al-Garadi, K.; Elkatatny, S. Impact of Methane Adsorption on Tight Rock Permeability Measurements Using Pulse-Decay. *Petroleum* **2019**, *5* (4), 382−387.

(36) Langmuir, I. The Adsorption of Gases on Plane Surfaces of Glass, Mica and Platinum. *J. Am. Chem. Soc.* **1918**, *40* (9), 1361−1403.

(37) Guarín Romero, J.; Moreno-Piraján, J.; Giraldo Gutierrez, L. Kinetic and Equilibrium Study of the Adsorption of CO2 in Ultramicropores of Resorcinol-Formaldehyde Aerogels Obtained in Acidic and Basic Medium. *C* **2018**, *4* (4), 52.

https://doi.org/10.1021/acsomega.3c04615
ACS Omega 2023, 8, 42329−42339

(38) Kalam, S.; Abu-Khamsin, S. A.; Kamal, M. S.; Patil, S. Surfactant Adsorption Isotherms: A Review. *ACS Omega* **2021**, *6* (48), 32342−32348.
(39) Douven, S.; Paez, C. A.; Gommes, C. J. The Range of Validity of Sorption Kinetic Models. *J. Colloid Interface Sci.* **2015**, *448*, 437−450.
(40) Mane, V. S.; Deo Mall, I.; Chandra Srivastava, V. Kinetic and Equilibrium Isotherm Studies for the Adsorptive Removal of Brilliant Green Dye from Aqueous Solution by Rice Husk Ash. *J. Environ. Manage.* **2007**, *84* (4), 390−400.
(41) Piccin, J. S.; Dotto, G. L.; Pinto, L. A. A. Adsorption Isotherms and Thermochemical Data of FDandC RED N° 40 Binding by Chitosan. *Brazilian J. Chem. Eng.* **2011**, *28* (2), 295−304.
(42) Kapoor, A.; Yang, R. T. Correlation of Equilibrium Adsorption Data of Condensible Vapours on Porous Adsorbents. *Gas Sep. Purif.* **1989**, *3* (4), 187−192.
(43) Deng, H.; Yi, H.; Tang, X.; Yu, Q.; Ning, P.; Yang, L. Adsorption Equilibrium for Sulfur Dioxide, Nitric Oxide, Carbon Dioxide, Nitrogen on 13X and 5A Zeolites. *Chem. Eng. J.* **2012**, *188*, 77−85.
(44) Du, X.; Cheng, Y.; Liu, Z.; Yin, H.; Wu, T.; Huo, L.; Shu, C. CO2 and CH4 Adsorption on Different Rank Coals: A Thermodynamics Study of Surface Potential, Gibbs Free Energy Change and Entropy Loss. *Fuel* **2021**, *283*, No. 118886. June 2020
(45) Song, X.; Wang, L.; Ma, X.; Zeng, Y. Adsorption Equilibrium and Thermodynamics of CO 2 and CH 4 on Carbon Molecular Sieves. *Appl. Surf. Sci.* **2017**, *396*, 870−878.
(46) Zou, M.; Wei, C.; Zhang, M.; Shen, J.; Chen, Y.; Qi, Y. Classifying Coal Pores and Estimating Reservoir Parameters by Nuclear Magnetic Resonance and Mercury Intrusion Porosimetry. *Energy Fuels* **2013**, *27* (7), 3699−3708.
(47) Gensterblum, Y.; Merkel, A.; Busch, A.; Krooss, B. M. High-Pressure CH4 and CO2 Sorption Isotherms as a Function of Coal Maturity and the Influence of Moisture. *Int. J. Coal Geol.* **2013**, *118*, 45−57.
(48) Crosdale, P. J.; Beamish, B. B.; Valix, M. Coalbed Methane Sorption Related to Coal Composition. *Int. J. Coal Geol.* **1998**, *35* (1−4), 147−158.
(49) Mangi, H. N.; Chi, R.; DeTian, Y.; Sindhu, L.; Lijin; He, D.; Ashraf, U.; Fu, H.; Zixuan, L.; Zhou, W.; Anees, A. The Ungrind and Grinded Effects on the Pore Geometry and Adsorption Mechanism of the Coal Particles. *J. Nat. Gas Sci. Eng.* **2022**, *100*, No. 104463. February
(50) Roy, M. Studies on Coal Macerals. III. Aerial Oxidation of Macerals. *Econ. Geol.* **1965**, *60*, 1213−1217.
(51) Abunowara, M.; Bustam, M. A.; Sufian, S.; Eldemerdash, U. Characterization of Malaysian Coals for Carbon Dioxide Sequestration. *IOP Conf. Ser.: Earth Environ. Sci.* **2016**, *36* (1), No. 114905.
(52) Mangi, H. N.; Detian, Y.; Hameed, N.; Ashraf, U.; Rajper, R. H. Pore Structure Characteristics and Fractal Dimension Analysis of Low Rank Coal in the Lower Indus Basin, SE Pakistan. *J. Nat. Gas Sci. Eng.* **2020**, *77*, No. 103231. October 2019
(53) Ping, A.; Xia, W.; Peng, Y.; Xie, G. Comparative Filtration and Dewatering Behavior of Vitrinite and Inertinite of Bituminous Coal: Experiment and Simulation Study. *Int. J. Min. Sci. Technol.* **2021**, *31* (2), 233−240.
(54) Teng, J.; Mastalerz, M.; Hampton, L. B. Maceral Controls on Porosity Characteristics of Lithotypes of Pennsylvanian High Volatile Bituminous Coal: Example from the Illinois Basin. *Int. J. Coal Geol.* **2017**, *172*, 80−94.
(55) Chen, X.; Wang, X.; Zhao, S.; Kang, N.; Feng, S. Effect of Moisture on Methane Adsorption Characteristics of Long-Flame Coal. *ACS Omega* **2022**, *7*, 16670.
(56) Rong, L.; Xiao, J.; Wang, X.; Sun, J.; Jia, F.; Chu, M. Low-Rank Coal Drying Behaviors under Negative Pressure: Thermal Fragmentation Volume Shrinkage and Changes in Pore Structure. *J. Clean. Prod.* **2020**, *272*, No. 122572.
(57) Nie, B.; Liu, X.; Yang, L.; Meng, J.; Li, X. Pore Structure Characterization of Different Rank Coals Using Gas Adsorption and Scanning Electron Microscopy. *Fuel* **2015**, *158*, 908−917.
(58) Pujobroto, A. *Organic Petrology and Geochemistry of Bukit Asam Coal*; Univ. Wollongong Thesis Collect: South Sumatra, Indonesia, 1997.

https://doi.org/10.1021/acsomega.3c04615
ACS Omega 2023, 8, 42329−42339